Subtleties in the averaging of a class of hybrid systems with applications to power converters

Luigi Iannelli [a] Karl Henrik Johansson [b] Ulf T. Jönsson [c]
Francesco Vasca [a]

[a] *Dept. of Engineering, University of Sannio, Benevento, Italy*

[b] *School of Electrical Engineering, Royal Institute of Technology, Stockholm, Sweden*

[c] *Division of Optimization and Systems Theory, Royal Institute of Technology, Stockholm, Sweden*

Abstract

High-frequency dither signals are commonly used to implement modulation schemes in power electronics converters. These systems represent an interesting class of hybrid systems with external excitation. They have a rich dynamical behaviour, which cannot be easily understood intuitively. Despite the common use of averaging techniques in power electronics, it was only recently proved that a dithered hybrid system can be approximated by an averaged system under certain conditions on the dither signal. Averaging and averaged models for various types of power converters are analyzed in the paper. It is shown that the averaged nonlinearity depends on the dither shape and that dither signals with Lipschitz-continuous averaged nonlinearities can be used to adapt the equivalent gain of power converters. Practical stability of the original dithered system can be inferred by analyzing a simpler averaged system. The main contribution of the paper is to show that the averaged and the dithered systems may have drastically different behavior if the assumptions of the recently developed averaging theory for dithered hybrid systems are violated. Several practical experiments and simulation examples of power electronics converters are discussed. They indicate that the conditions on the dither signal imposed by the averaging theory are rather tight.

Key words: Averaging; dither; power converters; hybrid systems.

⋆ The work by L. Iannelli and F. Vasca was supported by the European Commission within the SICONOS project IST2001-37172. The work by K. H. Johansson and U. Jönsson was supported by the European Commission within the Network of Excellence HYCON and by the Swedish Research Council. K. H. Johansson was also supported by the Swedish Foundation for Strategic Research through an INGVAR grant.

1 Introduction

Many power electronics systems have switching devices that more or less instantaneously change the dynamics of the system. Ideal models of diodes and controlled switches give rise to a class of hybrid dynamical systems, which consist of differential equations with discontinuous nonlinearities and external excitation signals. The understanding of the dynamical behavior of these systems is important to enable the design of more robust and efficient power converters, e.g., (Kassakian *et al*., 2001; Banerjee and Verghese, 2001).

Detailed analysis of hybrid models of power converters is difficult due to potentially complex interaction between the nonsmooth dynamics and the external carrier signal. Such signal, which is here interpreted as the dither, determines the commutations of the switches by means of a comparison with a suitable modulation signal. A possible approach to circumvent some of the difficulties is to average the hybrid dynamics over the period of the carrier signal. If the dither is of sufficiently high frequency, the behavior of the averaged system will often be close to the original system. Although the averaging approach is widely used in practice (Mohan *et al*., 1995), only recently rigorous averaging analysis was introduced, e.g., (Lehman and Bass, 1996). For a general class of Lipschitz-continuous systems, the averaging approach was theoretically justified by Zames and Shneydor already in the 1970s (Zames and Shneydor, 1976; Zames and Shneydor, 1977). They considered a class of feedback systems with linear dynamics and Lipschitz-continuous static nonlinearities excited by a dither signal, and showed that the amplitude distribution function of the dither plays a key role in understanding the stabilizing effect of the dither on the closed-loop system. The assumption on Lipschitz continuity posed by Zames and Shneydor is however often violated in practice; for example, that is the case for several power converters controlled using pulse width modulation. Results were recently obtained on averaging and stability for dithered systems with nonsmooth dynamics (Gelig and Churilov, 1998; Iannelli *et al*., 2003; Teel *et al*., 2004; Iannelli *et al*., 2006). When the dynamics are nonsmooth, it seems like there is a considerably smaller class of dither signals that can be used, compared to the smooth case considered by Zames and Shneydor. For instance, the averaging result in (Iannelli *et al*., 2006) requires the averaged system to be Lipschitz continuous, which, in the case of nonsmooth dynamics, in general means that the dither should have Lipschitz-continuous amplitude distribution function.

The main contribution of this paper is to show that when certain conditions on the carrier signal in power converters are violated, then averaging may fail to predict the correct system behavior. This finding is illustrated through a number of examples, by simulated models of DC/DC and three-phase converters as well as by two experimental set-ups of DC/DC converters. The results show the importance of some mathematical details behind the averaging theory: the sufficient conditions on the dither, first presented in (Iannelli *et al*., 2006), are rather tight, and

disregarding them could have a dramatic effect on the accuracy of the averaging. It is also indicated how averaging can be used to infer rigorous practical stability of the dithered system by analyzing the simpler averaged system, cf., (Gelig and Churilov, 1998; Moreau and Aeyels, 2000; Iannelli *et al*., 2003).

The outline of the paper is as follows. Section 2 presents four common types of switched power converters. They can all be represented as a particular class of hybrid systems with external dither excitation. Section 3 presents some background on the averaging for this class of hybrid systems. Practical stability results on the dithered system derived by assuming exponential stability of the averaged system are presented in Section 4. How to choose the shape of the dither is discussed in Section 5. Disregarding certain conditions on the dither signal can give rise to interesting dynamical phenomena, which are discussed in Section 6. They can also be verified in reality, so Section 7 confirms the theory through power converter experiments. The paper is concluded in Section 8 with some future directions.

2 A hybrid model for a class of switched power converters

This section considers switched power converters composed of linear passive electrical components (resistors, inductors, capacitors), independent voltage and current sources, and ideal diodes, transistors, and thyristors. As examples DC/DC buck and boost converters, an H-bridge drive, and a three-phase converter are discussed. The section is concluded by showing that these converters, when operating in continuous conduction mode, can be modeled using the same class of hybrid models.

2.1 DC/DC buck converter

The circuit diagram of a voltage-mode controlled buck converter is reported in Fig. 1. The purpose of this converter is to reduce the input voltage v to a desired output value, say x_2^{ref}, without large energy losses. By choosing as state variables the inductor current x_1, the capacitor voltage x_2 and the output x_3 of the integral block of the controller, the dynamic model of the converter under continuous conduction mode (i.e., the current through the inductor is assumed to be always positive) can be represented as

$$\dot{x}(t) = A_0 x(t) + b_0 r(t) + b_1 v(t)\, n(k_p r(t) - c x(t) - \delta(t)) \tag{1}$$

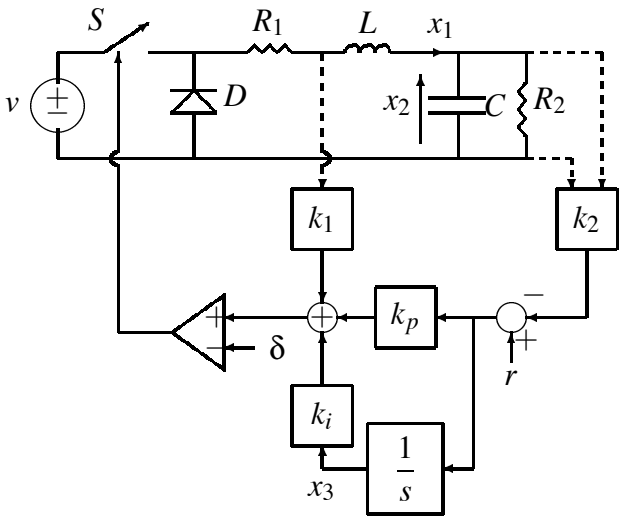

Fig. 1. DC/DC buck converter under voltage-mode control: S represents an ideal switch, D is an ideal diode, δ is the dither signal, and k_1, k_2, k_p, k_i are the control parameters.

with

$$A_0 = \begin{bmatrix} -R_1/L & -1/L & 0 \\ 1/C & -1/(R_2C) & 0 \\ 0 & -k_2 & 0 \end{bmatrix}, \quad b_0 = \begin{bmatrix} 0 \\ 0 \\ 1 \end{bmatrix}, \quad b_1 = \begin{bmatrix} 1/L \\ 0 \\ 0 \end{bmatrix}, \quad c = \begin{bmatrix} -k_1 & k_2k_p & -k_i \end{bmatrix}$$

where k_1 and k_2 are the state feedback gains, $r = k_2 x_2^{\text{ref}}$, k_p and k_i are the gains of the proportional and integral terms of the controller, respectively, and δ is the periodic carrier signal (typically, a sawtooth signal). The step nonlinearity n is given by

$$n(z) = \begin{cases} 1, & z > 0 \\ 0, & z < 0, \end{cases} \tag{2}$$

and the switch S is assumed to be a short circuit (and D an open circuit) if $n(z) = 1$ and an open circuit (and D a short circuit) if $n(z) = 0$. A model of the open-loop modulated power converter is simply obtained from (1) by letting $k_1 = k_2 = k_i = 0$.

2.2 H-bridge drive

A power electronic drive with a position-controlled DC motor and a full bridge, or H-bridge, DC/DC converter is shown in Fig. 2. The control objective for the system is to put the motor shaft at a desired angular position x_1^{ref}. The angular position of the shaft x_1 is measured by using a rotational potentiometer with gain k_{pot}, therefore $r = k_{\text{pot}} x_1^{\text{ref}}$. The motor supply voltage is obtained through a bipolar modulation of the DC/DC converter: when the pair (S_1^+, S_2^-) is conducting, the voltage over the

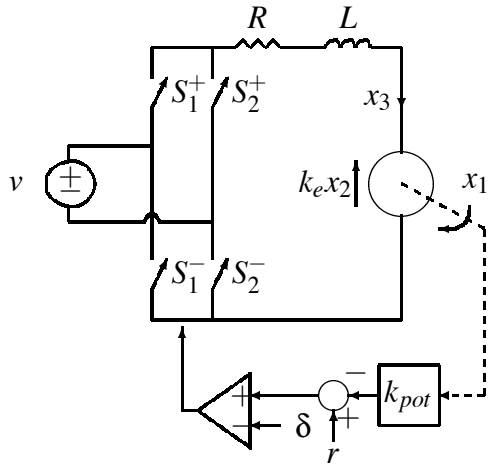

Fig. 2. Position controlled DC motor driven by a H-bridge power converter: $S_{1,2}^{\pm}$ represent ideal switches, δ is the dither signal, k_{pot} is the transducer gain and k_e is the electromagnetic constant.

DC motor is v, and when (S_1^-, S_2^+) is conducting, the voltage over the DC motor is $-v$. By introducing as state vector, the angular position x_1, the angular speed x_2, and the armature current x_3, the dynamic model of the power electronic system can be represented as

$$\dot{x}(t) = A_0 x(t) + b_0 v(t) + b_1 v(t)\, n(r(t) - cx(t) - \delta(t)) \tag{3}$$

with

$$A_0 = \begin{bmatrix} 0 & 1 & 0 \\ 0 & -\beta/J & k_t/J \\ 0 & -k_e/L_a & -R_a/L_a \end{bmatrix}, \quad b_0 = \begin{bmatrix} 0 \\ 0 \\ -1/L_a \end{bmatrix}, \quad b_1 = -2b_0, \quad c = \begin{bmatrix} k_{\text{pot}} & 0 & 0 \end{bmatrix}$$

where β is the friction coefficient, J the motor inertia, k_t the torque constant, k_e the electromagnetic constant, R_a the armature resistance, L_a the armature inductance. It is assumed that when $n(z) = 1$ the pair (S_1^+, S_2^-) is conducting and when $n(z) = 0$ the pair (S_1^-, S_2^+) is conducting.

2.3 DC/DC boost converter

A DC/DC boost converter generates at steady state an average output voltage that is larger than its input voltage. The boost converter reported in Fig. 3 can be modeled as

$$\dot{x}(t) = A_0 x(t) + b_0 v(t) + A_1 x(t)\, n(r(t) - cx(t) - \delta(t)), \tag{4}$$

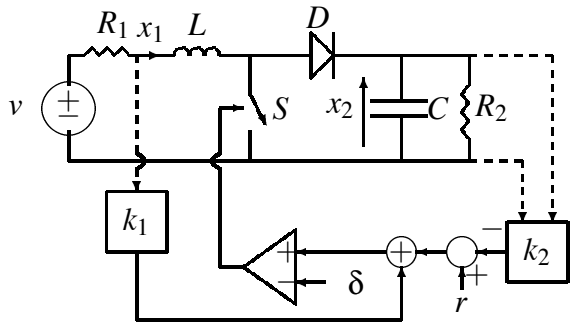

Fig. 3. DC/DC boost converter under voltage-mode control: S represents an ideal switch, D is an ideal diode, δ is the dither signal and k_1, k_2 are the control parameters.

with

$$A_0 = \begin{bmatrix} -R_1/L & -1/L \\ 1/C & -1/(R_2C) \end{bmatrix}, \; A_1 = \begin{bmatrix} 0 & 1/L \\ -1/C & 0 \end{bmatrix}, \; b_0 = \begin{bmatrix} 1/L \\ 0 \end{bmatrix}, \; c = \begin{bmatrix} -k_1 & k_2 \end{bmatrix}.$$

The notation is similar to the buck converter, so δ is a periodic carrier signal, n denotes the step function, S is conducting when $n(z) = 1$ etc. Note that in the boost converter model (4), as opposed to the previous models (1) and (3), the nonlinearity n multiplies the state variables.

2.4 Three-phase converter

Consider the three phase power converter reported in Fig. 4. Let us introduce for each lag $i = 1,2,3$, a corresponding control variable $\hat{u}_i$, which is equal to $+1$ if S_i^+ is conducting (and S_i^- is not) and -1 if S_i^- is conducting (and S_i^+ is not). By applying the Kirchhoff's circuit laws one obtains:

$$L\dot{x}_1(t) = -Rx_1(t) + v_1(t) - v_2(t) + Rx_2(t) + L\dot{x}_2(t) + \frac{-\hat{u}_1(t) + \hat{u}_2(t)}{2} x_4(t) \quad (5)$$

$$L\dot{x}_2(t) = -Rx_2(t) + v_2(t) - v_3(t) + Rx_3(t) + L\dot{x}_3(t) + \frac{-\hat{u}_2(t) + \hat{u}_3(t)}{2} x_4(t) \quad (6)$$

$$L\dot{x}_3(t) = -Rx_3(t) + v_3(t) - v_1(t) + Rx_1(t) + L\dot{x}_1(t) + \frac{-\hat{u}_3(t) + \hat{u}_1(t)}{2} x_4(t) \quad (7)$$

$$C\dot{x}_4(t) = \frac{\hat{u}_1(t)+1}{2} x_1(t) + \frac{\hat{u}_2(t)+1}{2} x_2(t) + \frac{\hat{u}_3(t)+1}{2} x_3(t) - \frac{1}{R_L} x_4(t). \quad (8)$$

By using the equilibrium condition for the currents $x_1(t) + x_2(t) + x_3(t) \equiv 0$, one can substitute $\dot{x}_2(t) = -\dot{x}_1(t) - \dot{x}_3(t)$ in (5), and by using (7) together with the (typical)

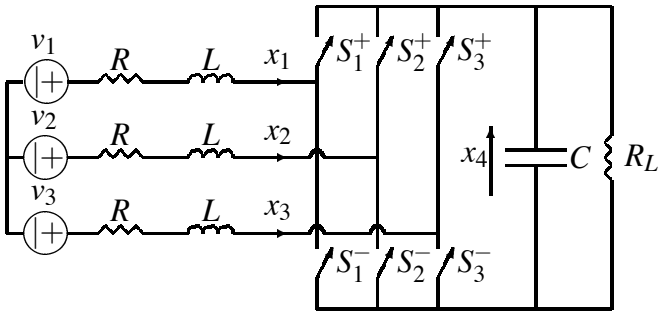

Fig. 4. Three phase power converter: $S^{\pm}_{1,2,3}$ represent ideal switches.

equilibrium condition for the input voltages, $v_1(t)+v_2(t)+v_3(t)=0$, equation (5) can be rewritten as

$$L\dot{x}_1(t) = -Rx_1(t) + v_1(t) + \frac{1}{6}(-2\hat{u}_1(t) + \hat{u}_2(t) + \hat{u}_3(t))x_4(t).$$

With similar arguments one can write

$$\begin{aligned}
L\dot{x}_2(t) &= -Rx_2(t) + v_2(t) + \frac{1}{6}(\hat{u}_1(t) - 2\hat{u}_2(t) + \hat{u}_3(t))x_4(t) \\
L\dot{x}_3(t) &= -Rx_3(t) + v_3(t) + \frac{1}{6}(\hat{u}_1(t) + \hat{u}_2(t) - 2\hat{u}_3(t))x_4(t) \\
C\dot{x}_4(t) &= \frac{1}{2}\hat{u}_1(t)x_1(t) + \frac{1}{2}\hat{u}_2(t)x_2(t) + \frac{1}{2}\hat{u}_3(t)x_3(t) - \frac{1}{R_L}x_4(t).
\end{aligned}$$

The commutation of the switches can be determined by means of a modulated state feedback. Then the signals $\hat{u}_i$ can be written as

$$\hat{u}_i(t) = 2n(r_i(t) - c_i x(t) - \delta(t)) - 1,$$

where $n(z_i) = 1$ (respectively, $n(z_i) = 0$) means that, the upper (lower) switch of the i-th lag is conducting. Thus, the entire model of the controlled converter can be written as

$$\dot{x}(t) = A_0 x(t) + b_0 v(t) + \sum_{i=1}^{3} A_i x(t)\; n(r_i(t) - c_i x(t) - \delta(t)) \tag{9}$$

where v is the vector of the input voltages, A_0, A_i and b_0 are matrices that can be derived from the previous equations, and c_i depend on the control strategy. A typical open loop modulation strategy consists of choosing δ as a triangular dither and r_i as low frequency sinusoidal signals with suitable phase shifts.

2.5 Hybrid model

General hybrid models, such as hybrid automata and switched systems, applicable for power converters but also for many other applications, are widely considered in the literature, e.g., (Lygeros *et al.*, 2003; Guéguen and Zaytoon, 2004; Liberzon, 2003). The converters presented above are examples of a rather wide class of power converters that can be modeled in the following form

$$\dot{x}(t) = A_0 x(t) + b_0 v(t) + \sum_{i=1}^{m} \left(A_i x(t) + b_i v(t)\right)\, n(r_i(t) - c_i x(t) - \delta(t)), \qquad (10)$$

where A_i, b_i and c_i are constant matrices of appropriate dimensions and m is an integer related to the number of modes of the converter. The initial condition $x(0)$ is denoted by x_0. The external input vector v and reference signals r_i are assumed to be Lipschitz continuous. The external carrier signal δ is assumed to be a high-frequency signal of period p. Here δ is called a dither signal and consequently the hybrid system (10) is called a dithered system. This terminology is frequently used for a variety of mechanical and electrical control systems with high-frequency excitation signals. In power electronics systems, δ is usually a sawtooth or triangular signal, but in the following a general shape of the signal will be allowed. Indeed, also dither signals that are constant over non-vanishing time intervals, such as square-waves, saturated, and quantized signals, are sometimes used in applications.

Since the differential equation (10) has a discontinuous right-hand side (because n is discontinuous), it is important to make some comments on the existence and uniqueness of solutions. In the following it is assumed that (10) has at least one absolutely continuous solution $x(t, x_0)$ on $[0, \infty)$ (in the sense of Carathéodory). It is supposed that the time intervals when the solution is at a discontinuity point of n are of zero Lebesgue measure. As a consequence, solutions with sliding modes are not considered. Furthermore, it is supposed that the solutions have no accumulation of switching events (Zeno solutions).

3 Averaging

In this section it is formulated a version of the main theorem in (Iannelli *et al.*, 2006), which will provide the foundation for the subsequent analysis. The averaged system corresponding to the dithered system (10) is defined as

$$\dot{w}(t) = A_0 w(t) + b_0 v(t) + \sum_{i=1}^{m} \left(A_i w(t) + b_i v(t)\right) N(r_i(t) - c_i w(t)) \qquad (11)$$

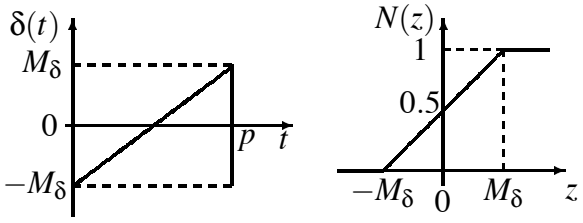

Fig. 5. Sawtooth dither and the corresponding averaged nonlinearity.

where $w(0) = x_0$ and N is an averaged nonlinearity, which is derived from the original step nonlinearity n and the dither signal δ as follows:

$$N(z) \triangleq \frac{1}{p}\int_{[0,p)} n(z-\delta(s))\mathrm{d}s. \tag{12}$$

The averaged nonlinearity obviously depends on the shape of δ. Typical dither signals are sawtooth, triangular, sinusoidal, trapezoidal, and square wave signals. Fig. 5 shows a sawtooth signal and its averaged nonlinearity. Note that triangular dither and sawtooth dither with the same amplitude and period have the same averaged nonlinearity.

The following averaging result follows from Theorem 3.1 in (Iannelli *et al.*, 2006). It states conditions when the dithered system (10) can be approximated by the averaged system (11).

Proposition 3.1 (Iannelli *et al.* (2006)) *Consider the dithered system* (10) *and the averaged system* (11) *under the following assumptions:*

(*i*) *the external signals $r(t)$ and $v(t)$ are Lipschitz continuous,*
(*ii*) *the dither δ is p-periodic, $|\delta| \le M_\delta$, and the corresponding averaged nonlinearity is Lipschitz continuous.*

Then, the averaged system (11) *has a unique absolutely continuous solution on $[0,\infty)$. Moreover, for any compact set $\mathcal{K} \subset \mathbb{R}^n$ and any $T > 0$, there exists a positive constant $\gamma = \gamma(\mathcal{K}, T)$ such that*

$$|x(t,x_0) - w(t,x_0)| \le \gamma p, \quad \forall x_0 \in \mathcal{K},\ t \in [0,T]. \tag{13}$$

The approximation error depends linearly on the dither period. The proof in (Iannelli *et al.*, 2006) is constructive and gives an estimate of γ that has exponential dependence on T but is independent of p. This fact can be used to derive an upper bound on the approximation error between the dithered and the averaged systems over an infinite time horizon provided that some stability condition is satisfied, see next section for such a result.

It is straightforward to extend the averaging theorem to the case of more than one dither signal (Iannelli *et al.*, 2006). In that case, the averaged system will have one

averaged nonlinearity corresponding to each dither. Moreover, it is possible to relax the periodicity assumption on the dither and instead consider dither signals that have some more general time repetition properties (Zames and Shneydor, 1976). See (Iannelli *et al*., 2004) for details on how to extend Proposition 3.1 in this case.

It is possible to characterize a dither signal using its amplitude distribution function (ADF). The ADF $F_\delta : \mathbb{R} \to [0,1]$ of a p-periodic dither signal $\delta : [0,\infty) \to \mathbb{R}$ is defined as

$$F_\delta(\xi) \triangleq \frac{1}{p}\mu\left(\{t \in [0,p) : \delta(t) \leq \xi\}\right),$$

where μ denotes the Lebesgue measure. The amplitude distribution function simply says how large fraction of each period the dither signal lies below the level ξ. The ADF is thus a deterministic analog of the probability distribution function. In particular, it is a bounded, monotonically increasing function that takes values in the interval $[0,1]$. The averaged nonlinearity corresponding to the step function is equal to the ADF of the dither:

$$N(z) = \frac{1}{p}\int_{[0,p)} n(z-\delta(s))\,\mathrm{d}s = \int_{\mathbb{R}} n(z-\xi)\,\mathrm{d}F_\delta(\xi) = \int_{-\infty}^{z} \mathrm{d}F_\delta(\xi) = F_\delta(z). \quad (14)$$

Therefore the averaged nonlinearity is determined by the shape of the dither. An alternative condition in (ii) of Proposition 3.1 is thus that the ADF should be Lipschitz continuous.

4 Stability analysis

Proposition 3.1 can be used to derive stability results for the dithered system. In this section it is shown that if the averaged system (11) has an exponentially stable equilibrium, then the dithered system is practically stable.

Proposition 4.1 *Suppose the averaged system (11) has an exponentially stable equilibrium at w^0, i.e., there exist $\alpha_0 > 0$ and $\beta_0 \geq 1$ such that*

$$|w(t) - w^0| \leq \beta_0 e^{-\alpha_0 t}|w(0) - w^0|, \quad \forall t \in [0,\infty).$$

If the conditions of Proposition 3.1 are satisfied, then for any compact set $\mathcal{K}$ and constants $\varepsilon > 0$ and $0 < \alpha < \alpha_0$, the dithered system (10) satisfies

$$|x(t) - w^0| \leq \beta_0 e^{-\alpha t}|x(0) - w^0| + \varepsilon, \quad \forall x(0) \in \mathcal{K},\ t \in [0,\infty)$$

for all $p \in (0, p_0)$ where

$$p_0 = \frac{1-\alpha_1}{(\beta_0 + (1-\alpha_1))\gamma}\varepsilon, \quad T = -\alpha_0^{-1}\ln(\alpha_1/\beta_0),$$

$\alpha_1 = \beta_0^{-\alpha/(\alpha_0-\alpha)} \in (0,1)$, *and* $\gamma = \gamma(\mathcal{K}, T)$ *as in Proposition 3.1.*

PROOF. See Appendix.

The result shows that the state of the dithered system converges to a neighbourhood of the origin with a rate similar to the averaged system, provided that the dither frequency is sufficiently high. The size of the neighborhood is determined by the high frequency ripple that appears due to the dither signal.

The relationship between the averaged and the dithered solutions show that dithering can be also interpreted as a technique for regularizing solutions of nonsmooth systems. In fact, since n is discontinuous, the solution of (10) might not be unique. On the other hand, if the averaged nonlinearity is Lipschitz, the averaged system (11) will have a unique solution. Now, from Proposition 3.1 and Proposition 4.1 one can conclude that by decreasing the dither period, all possible solutions of (10) will get closer and closer to the unique solution of the averaged system (11).

Proposition 4.1 assumes that the averaged system (11) has an exponentially stable equilibrium. Regarding the stability analysis of smooth averaged systems, there are many available results. Here stability conditions are considered for a class of averaged systems with $m = 1$, $v(t) = E$ constant, $r(t) = r$ constant, $b_0 = 0$, $A_1 = 0$, $b_1 = b/E$, and $A_0 = A$, where A is a Hurwitz matrix and b is a given vector. The averaged dynamics become

$$\dot{w}(t) = Aw(t) + bN(r - cw(t)). \tag{15}$$

From (15) the equilibrium state can be written as $w^0 = -A^{-1}bN(e_0)$ and the equilibrium value of the output error $e_0 = r - cw^0$ is determined by the equation

$$e_0 - cA^{-1}bN(e_0) = r. \tag{16}$$

The system (15) is on Luré form, i.e., it is a negative feedback interconnection between a linear system $G(s) = c(sI - A)^{-1}b$ and a static nonlinearity.

The averaged models of buck converters and H-bridge converters are on Luré form. The Popov criterion is one of many possible tools for proving exponential stability of such systems. More sophisticated results include the Zames and Falb (1968) result and the integral quadratic constraint method (Megretski and Rantzer, 1997). By using the Popov criterion, the following proposition provides conditions for the exponential stability of the averaged system (15).

Proposition 4.2 *The equilibrium* $w^0 = -A^{-1}bN(e_0)$ *of (15), where* e_0 *satisfies (16), is exponentially stable with rate of decay* $\alpha > 0$*, if there exists* $k > 0$ *such that*

(*i*) $A + \alpha I$ *is Hurwitz,*
(*ii*) N *is in the sector* $[0,k]$*, i.e.,*

$$(e - e_0 - \frac{1}{k}(N(e) - N(e_0)))(N(e) - N(e_0)) \geq 0, \quad \forall e \in \mathbb{R},$$

(*iii*) *there exists* $\lambda \geq 0$ *such that*

$$\mathrm{Re}\,((1 + \lambda(j\omega - \alpha)G(j\omega - \alpha)) \geq \alpha\lambda k|G(j\omega - \alpha)|^2 - \frac{1}{k}, \quad \forall \omega \in \mathbb{R}.$$

PROOF. See Appendix.

Proposition 4.2 illustrates how it is possible to infer stability of the dithered system by analyzing the simpler averaged system. In next section it is shown how the result can be used to predict the behavior of a buck converter. Proposition 4.2 can be extended to the case when there is integral action in the dynamics (Jönsson and Megretski, 2000).

Many converter models such as the boost converter and the three phase converter do not have averaged dynamics on Luré form. These systems have instead bilinear averaged dynamics. In general, it is easier to analyze these systems with Lagrangian and Hamiltonian methods, e.g., (Ortega *et al.*, 1988; Escobar *et al.*, 1999).

5 Effects of dither shape

The results on averaging and stability show that robustness and stability properties satisfied by the averaged system can be inherited by the dithered system. This section gives some examples that illustrate how the dither can be used for designing control systems and motivate the need for a deeper investigation of the possible use of dither shapes.

5.1 Stabilization through appropriate dither

Consider the DC/DC buck converter under proportional control and sawtooth dither (see Fig. 1). The controller parameters are $k_1 = 0$, $k_2 = 1$, $k_p = 0.5$, $k_i = 0$, and

$v(t) = E$ constant. The averaged dynamics can be written in the form (15) with

$$A = \begin{bmatrix} -R_1/L & -1/L \\ 1/C & -1/(R_2C) \end{bmatrix}, \quad b = \begin{bmatrix} E/L \\ 0 \end{bmatrix}, \quad c = \begin{bmatrix} 0 & 0.5 \end{bmatrix},$$

and the averaged nonlinearity is

$$N(z) = \begin{cases} 1, & z > M_\delta \\ 0.5 + z/(2M_\delta), & |z| \le M_\delta \\ 0, & z < -M_\delta, \end{cases}$$

which belongs to the sector $[0, 1/(2M_\delta)]$. If $e_0 \in [-M_\delta, M_\delta]$, then $N(e_0) = 0.5 + e_0/(2M_\delta)$ and (16) gives

$$e_0 = \frac{2M_\delta(r - 0.5G(0))}{2M_\delta + G(0)},$$

where $G(s) = c(sI - A)^{-1}b$. Hence, provided that $e_0 \in [-M_\delta, M_\delta]$, it follows that the stationary output error is

$$x_2^{\text{ref}} - w_2^0 = \frac{2M_\delta(r - 0.5G(0))}{0.5(2M_\delta + G(0))} \tag{17}$$

and the stability condition (iii) of Proposition 4.2 is

$$\text{Re}\,((1 + \lambda(j\omega - \alpha)G(j\omega - \alpha)) \ge \frac{\alpha\lambda}{2M_\delta}|G(j\omega - \alpha)|^2 - 2M_\delta, \quad \forall \omega \in \mathbb{R}. \tag{18}$$

It follows that the stationary output error becomes smaller as the dither amplitude M_δ is decreased. The loop gain is in the linear range of the nonlinearity inversely proportional to M_δ, which implies a faster response as M_δ decreases. The price paid for a higher loop gain is that the stability criterion in (18) is harder to satisfy. It may seem contradictory to get a higher loop gain, and thus faster dynamics, at the same time as a smaller rate of decay α is needed in (18). The reason is that the stability criterion provides a global estimate of the rate of convergence and takes the saturation into account in the estimate.

Consider the following converter parameters $R_1 = 0.1\Omega$, $L = 10\,\text{mH}$, $C = 220\,\mu\text{F}$, $R_2 = 8.9\,\Omega$, $E = 10\,\text{V}$. By computing the stationary output voltage in (17) and an upper bound for α in the stability criterion in (18), the following table can be obtained:

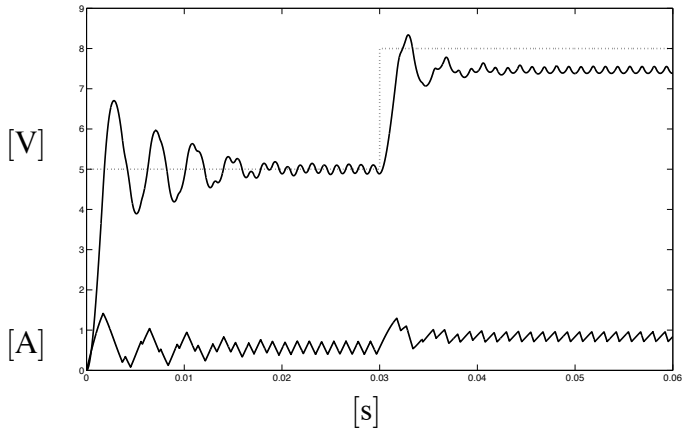

Fig. 6. Capacitor voltage and inductor current of the closed loop DC/DC buck converter with triangular dither. The reference x_2^{ref} varies from 5 V to 8 V after 0.03 s. The dither period is $p = 1.25\,\mathrm{ms}$ with amplitude $M_\delta = 0.5$.

$x_2^{\mathrm{ref}} - w_2^0$	$M_\delta = 0.5$	$M_\delta = 5$
$x_2^{\mathrm{ref}} = 5$	0.01	0.04
$x_2^{\mathrm{ref}} = 8$	0.51	2.04
	$\alpha = 87$	$\alpha = 244$

These theoretical predictions are confirmed in the simulation experiments reported in Figs. 6–7. Note that by increasing the amplitude of the sawtooth dither signal, the stationary output voltage error increases at the same time as the rise time becomes larger. This is particularly easy to see when the reference voltage varies at $t =$ 0.03 s. Moreover the oscillations decay slower for a small amplitude of the dither. This is predicted by the smaller value of α.

5.2 Dithers with non-Lipschitz ADF

The dither shape can be designed to give a desired behavior of the averaged system. Consider, for instance, a system with triangular dither. Then the averaged nonlinearity is a saturation. If the averaged system is not stable in a neighborhood of the origin due to the high gain of the averaged nonlinearity, then it is possible to increase the amplitude of the dither and thus decrease the gain in the linear region of the nonlinearity, cf., Fig. 5. As an alternative, it is also possible to choose the dither shape so that the slope of the averaged nonlinearity is distributed unevenly over the nonsaturated region. One such possibility is to use a sinusoidal dither, which gives an averaged nonlinearity with small slope near the equilibrium at the expense of a steeper slope close to the saturation region, see Fig. 8. The averaged nonlinearity is

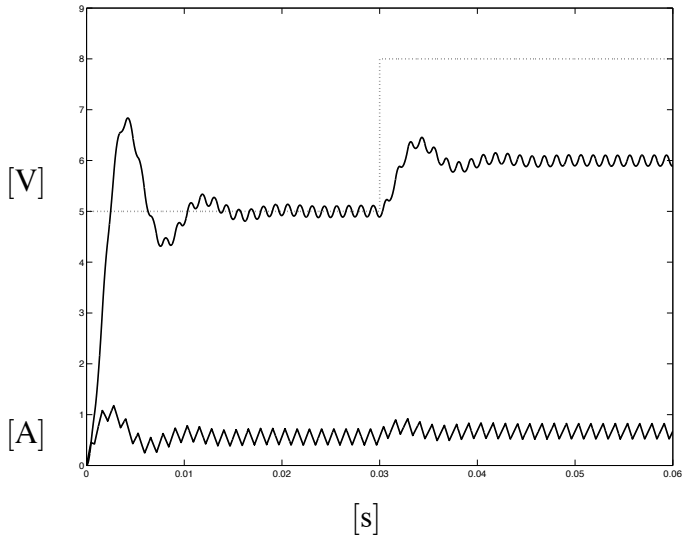

Fig. 7. Capacitor voltage and inductor current of the closed loop DC/DC buck converter with triangular dither. The converter and controller parameters are the same as in Fig. 6, but the dither amplitude is ten times larger ($M_\delta = 5$).

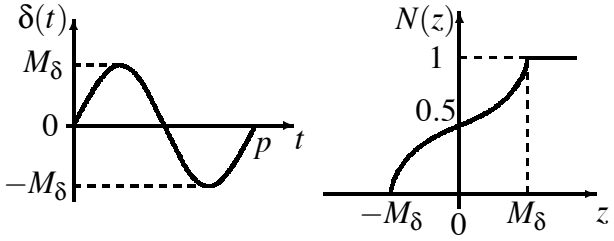

Fig. 8. Sinusoidal dither and the corresponding averaged nonlinearity.

in this case

$$N(z) = \begin{cases} 0 & z < -M_\delta \\ \frac{1}{2}\left(1 + \frac{2}{\pi}\sin^{-1}(\frac{z}{M_\delta})\right) & |z| \le M_\delta \\ 1 & z > M_\delta. \end{cases}$$

Note that $N(z)$ is continuous but not globally Lipschitz, so it does not satisfy condition (ii) of Proposition 3.1. It is nevertheless sometimes possible to successfully use this type of nonlinearity in applications to stabilize the system. An experimental example is given in Section 7. This motivates a further investigation of the need for the assumptions made on the dither signal in Proposition 3.1. In Section 6 it will be proven that if the condition (ii) in Proposition 3.1 is violated, then the averaged system does not necessarily approximate the dithered system. The averaged nonlinearity corresponding to the sinusoidal dither is continuous but has unbounded derivative. It is also possible to have discontinuous averaged nonlinearities. Since $n(z)$ is discontinuous in $z = 0$, it holds that if $\delta(t)$ is constant, equal to $\bar{\delta}$, say, for some nonzero time interval, then $N(z)$ is not defined for $z = -\bar{\delta}$. One such exam-

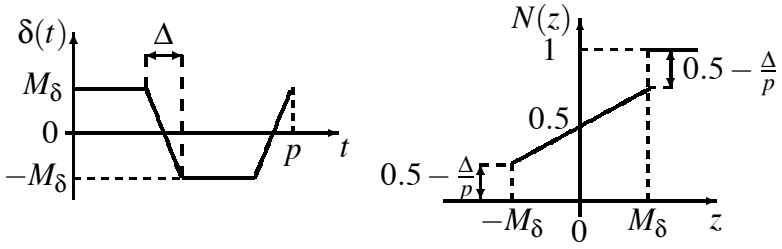

Fig. 9. Trapezoidal dither and the corresponding averaged nonlinearity; a square wave dither corresponds to $\Delta = 0$.

ple is the trapezoidal signal in Fig. 9. It is easy to see that dither signals that are constant over non-vanishing time intervals, such as trapezoidal and square wave signals, have discontinuous averaged nonlinearities. This class of *zero-slope* dither signals can give rise to interesting dynamical behaviors when applied to discontinuous feedback systems. They need to be carefully analyzed, as discussed in next section.

6 Subtleties in the averaging of switched power converters

This section shows that when conditions on the ADF are not satisfied, it is possible to find systems for which the conclusions of Proposition 3.1 do not hold. In particular it is shown that when conditions on the averaged nonlinearity are not satisfied, it can happen that there are multiple solutions of the averaged system, or an approximation error that cannot be arbitrarily decreased by increasing the dither frequency. The proofs of these results are constructive in the sense that they are based on examples that illustrate the limitations.

The following example shows that it cannot be ensured the existence of a unique solution to the averaged system unless it is imposed the boundedness of the derivative of the averaged nonlinearity $N(z)$. Consider the dithered nonsmooth feedback system (10) with $m = 1, A_0 = A_1 = 0, b_0 = 0, b_1 = 4, c_1 = -1, x(0) = -1, r_1(t) \equiv 0$, $v(t) \equiv 1$ and δ is the following p-periodic quadratic dither signal

$$\delta(t) = \begin{cases} -4M_\delta \left(\dfrac{t}{p}\right)^2 + M_\delta, & t \bmod p \in (0, \dfrac{p}{2}] \\ 4M_\delta \left(\dfrac{t}{p}\right)^2 - 8M_\delta \dfrac{t}{p} + 3M_\delta, & t \bmod p \in (\dfrac{p}{2}, p]. \end{cases}$$

The corresponding averaged nonlinearity is

$$N(z) = \begin{cases} 0 & z \le -M_\delta \\ \frac{1}{2}\sqrt{1+\frac{z}{M_\delta}} & -M_\delta \le z \le 0 \\ 1-\frac{1}{2}\sqrt{1-\frac{z}{M_\delta}} & 0 \le z \le M_\delta \\ 1 & z \ge M_\delta. \end{cases} \tag{19}$$

Note that $N(z)$ is absolutely continuous but its derivative is not bounded. The averaged system (11) now reduces to

$$\dot{w}(t) = 4N(-w(t)), \quad w(0) = -1$$

where $N(z)$ is given by (19). Note that this averaged system is not globally Lipschitz because $N(z)$ is not globally Lipschitz. It is easy to show that when $M_\delta = 1$ the averaged system has a nonunique solution. In fact, there are infinitely many solutions parameterized by $\tau \in [0,\infty)$ and given by

$$w(t) = \begin{cases} -1 & 0 \le t \le \tau \\ (t-\tau)^2 - 1 & t \ge \tau. \end{cases}$$

Then it is possible to claim the following proposition.

Proposition 6.1 *Suppose the averaged nonlinearity $N(z)$ is absolutely continuous but its derivative is not bounded. Then there exists a dithered system* (10) *for which the corresponding averaged system* (11) *does not have a unique solution.*

The next example shows that if the averaged nonlinearity is not absolutely continuous then the uniform approximation property in (13) of Proposition 3.1 cannot be guaranteed. Consider the nonsmooth feedback system (10) with $m = 1$, and

$$A_0 = \begin{bmatrix} -1 & -1 \\ 0 & -2 \end{bmatrix},\ A_1 = \begin{bmatrix} 0 & 0 \\ 0 & 0 \end{bmatrix},\ b_0 = \begin{bmatrix} 0 \\ -1 \end{bmatrix},\ b_1 = \begin{bmatrix} 0 \\ 2 \end{bmatrix},\ c_1 = \begin{bmatrix} 1 & 0 \end{bmatrix}.$$

Let the external signals be constants: $r_1(t) = 0.5$ and $v(t) = 1$. The dither δ is a square wave signal with amplitude $M_\delta = 0.5$. The averaged system (11) has an averaged nonlinearity N as given in Fig. 9 with $\Delta = 0$ and $M_\delta = 0.5$.

Let the state space of the dithered and the averaged systems be partitioned into the following three regions, see Fig. 10:

- Region $\Omega_1 = \{x : x_1 < 0\}$. In this region $n(r_1 - c_1 x - \delta) = 1$. The dithered system coincides with the averaged system and they have dynamics $\dot{x} = A_0 x - b_0$. The equilibrium point is $P_1 = A_0^{-1} b_0 = (-0.5, 0.5)^T$.

- Region $\Omega_2 = \{x : x_1 > 1\}$. In this region $n(r_1 - c_1 x - \delta) = 0$. The dithered system coincides with the averaged system and they have dynamics $\dot{x} = A_0 x + b_0$. The equilibrium point is $P_2 = -A_0^{-1} b_0 = (0.5, -0.5)^T$.
- Region $\Omega_0 = \{x : 0 < x_1 < 1\}$ with subsets $\Omega_0^+ = \{x : 0 < x_1 < 1,\ x_2 > 0.5\}$ and $\Omega_0^- = \{x : 0 < x_1 < 1,\ x_2 < -0.5\}$. In Ω_0 the state does not affect the output of the step nonlinearity. The dithered system can be represented by the linear system

$$\dot{\zeta} = A_0 \zeta - b_0 u \tag{20}$$

  with u a periodic signal that switches between -1 (when $r_1 - \delta(t) = 0$) and 1 (when $r_1 - \delta(t) = 1$). The averaged system has an input equal to zero in this region, i.e., $\dot{w} = A_0 w$.

Consider $x(0) = w(0)$, with $0 < x_1(0) < 1, 0 < x_2(0) < 0.5$ and $x_1(0) > x_2(0)$. It is easy to show that the averaged trajectory will tend to the origin without leaving the set indicated for the possible initial conditions. The dithered trajectory will oscillate about the averaged solution. By considering the vector fields indicated in Fig. 10, it follows that the dithered trajectory cannot leave the set $\Omega_0 - \{\Omega_0^+ \bigcup \Omega_0^-\}$ but by crossing the segment $\{x :\ x_1 = 0,\ 0 \leq x_2 \leq 0.5\}$. Moreover in Ω_0 the solution of the dithered system can be represented as

$$x(t) = e^{A_0 t}(x(0) - \zeta_0) + \zeta_{ss}(t),$$

where ζ_{ss} is the steady-state p-periodic solution of (20) and

$$\zeta_0 = -(I - e^{A_0 p})^{-1} \int_0^p e^{A_0 (p-s)} b u(s) \mathrm{d}s.$$

Since A_0 is Hurwitz, $x(t)$ will converge to $\zeta_{ss}(t)$, which is a counter clockwise oscillation around the origin. It is always possible to choose a small enough dither period p such that $\zeta_{ss}(t)$ never intersects Ω_2, since $\zeta_{ss} \to 0$ when $p \to 0$. It is then clear that $x(t)$ eventually will cross the x_2 axis for some $0 \leq x_2 \leq 0.5$.

It is easy to see that the second orthant is an invariant set under the dynamics of the dithered and averaged systems. Moreover, since the system matrix A_0 is Hurwitz, the dithered solution $x(t)$ will tend toward the equilibrium point P_1.

The above example shows that the dithered and the averaged systems behave qualitatively different since they converge to two different points, P_1 and the origin, respectively. This is in contradiction to the inequality (13) of Proposition 3.1. Indeed, if the compact set $\mathcal{K}$ includes the origin, it would need to make p smaller and smaller the closer x_0 is to the origin (on the trajectory indicated in Fig. 10) in order to get the inequality satisfied, because it always exists a p such that (13) does not hold. Hence, there is no uniform bound on p that holds for all $x_0 \in \mathcal{K}$. Then it is possible to state the following proposition.

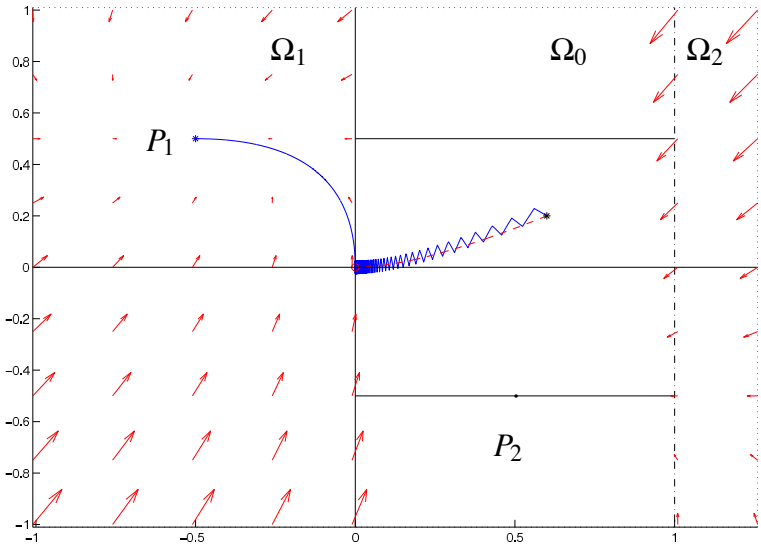

Fig. 10. Phase plane trajectories and vector fields for the dithered system (10) and the averaged system (11) with $p = 0.1$ and initial conditions $x_0 = w_0 = [0.6\ 0.2]^T$. The trajectory of the dithered system converges to P_1 while the trajectory of the averaged system converges to the origin.

Proposition 6.2 *Suppose the averaged nonlinearity $N(z)$ is discontinuous. Then there exists a dithered system* (10) *for which the uniform bound in* (13) *of Proposition 3.1 does not hold.*

The discrepancy between the averaged and the dithered dynamics indicated above have previously been discovered in simulations: limit cycles appeared in the dithered but not in the averaged system in an example in (Iannelli *et al.*, 2003). The second example in next section shows that such discrepancy also can appear under experimental conditions.

7 Experimental results

In this section experiments with the DC/DC buck converter and the H-bridge drive show how and when the averaging analysis can be used.

7.1 DC/DC buck converter

Consider the DC/DC buck converter reported in Fig. 1 with $R_1 = 0.1\Omega$, $L = 1$mH, $C = 220\mu$F, $R_2 = 8.9\Omega$, $r = 6$, $v = 10$V, $k_p = 0$, $k_1 = 0.5$, $k_2 = 1$, and $k_i = 10$. The controller is implemented through a dSPACE^{TM} DS1103 PPC controller board with a sampling period of 10μs. The implementation scheme of the controlled DC/DC buck converter is reported in Fig. 11.

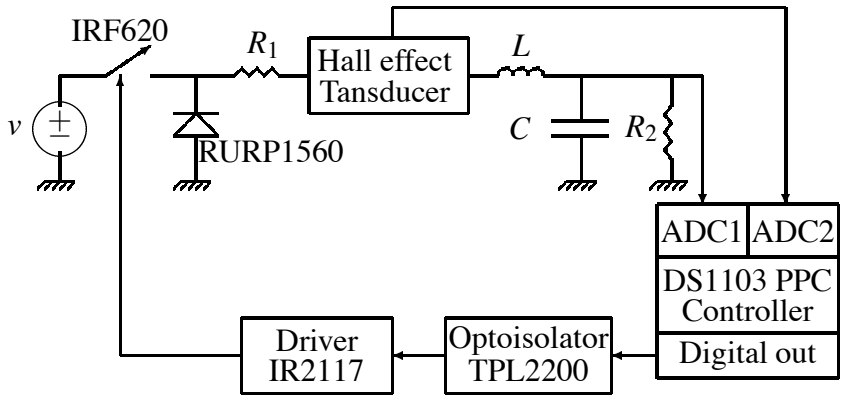

Fig. 11. Implementation scheme for the controlled DC/DC buck converter.

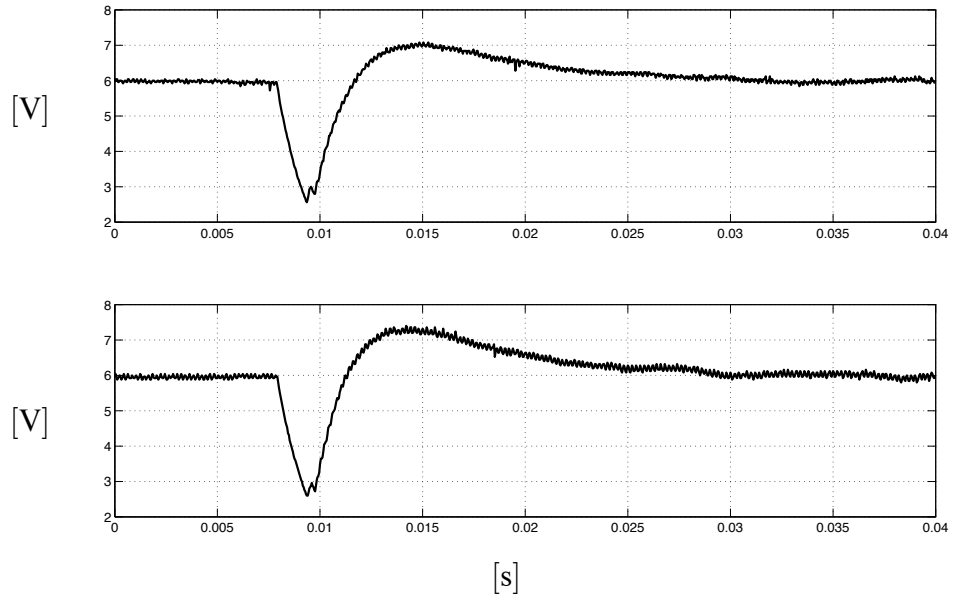

Fig. 12. Dynamic response of the output voltage to an input voltage variation (from 10V to 14V) for: (a) sawtooth dither (top diagram) and (b) sinusoidal dither (bottom diagram) both with $M_\delta = 0.25$ and $p = 200\mu$s. The sinusoidal dither leads to a slightly shorter rise time and a larger overshoot compared to the sawtooth dither.

The experimental results obtained by varying the input voltage from 10V to 14V using dither signals with different shapes and amplitudes are reported in Fig. 12 and Table 1.

Experiments show that the behavior of the controlled system is dependent on the dither shape and amplitude. For instance, for $M_\delta = 0.1$, the sinusoidal dither recovers the desired output voltage in a shorter time and with lower overshoot than the sawtooth dither signal. The opposite occurs for $M_\delta = 0.25$ (see Fig. 12) and $M_\delta = 0.35$. By computing the averaged models it is possible to verify that the experiments confirm that the dithered systems represent a good approximation of the

	Amplitude [V]	Settling time [ms]	Overshoot	Voltage ripple [V]
Sawtooth dither	0.1	15.6	18.3%	0.10
	0.25	15.0	18.2%	0.12
	0.35	14.8	18.7%	0.13
Sinusoidal dither	0.1	14.2	15.3%	0.12
	0.25	16.8	23.3%	0.15
	0.35	18.0	22.7%	0.16

Table 1
Experimental results of the DC/DC buck converter with input voltage change. The dither frequency is 5 kHz. The settling time is evaluated at 5% of the steady state averaged output voltage.

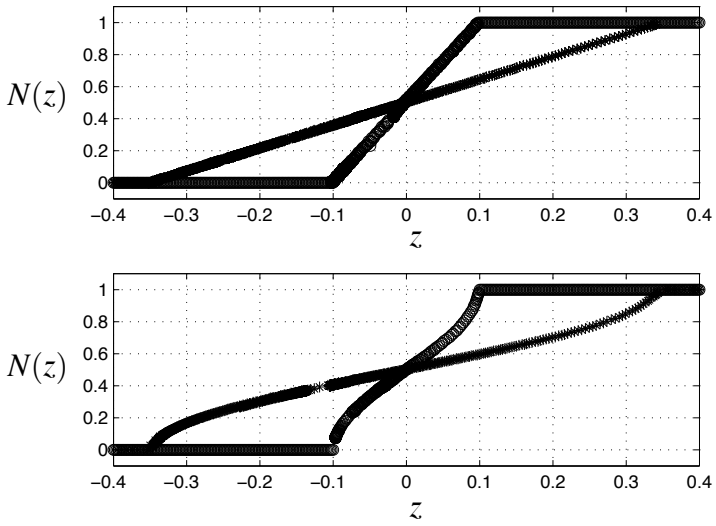

Fig. 13. Equivalent computed nonlinearity (with $p = 200\mu$s): (a) triangular dither (top diagram), (b) sinusoidal dither (bottom diagram) both with $M_\delta = 0.1, 0.35$. On the horizontal axis it is reported $z = \frac{1}{p}\int_{t-p}^{t}(r - cx(\tau) - \delta(\tau))d\tau$ and on the vertical axis it is reported $N(z) = \frac{1}{p}\int_{t-p}^{t} n(r - cx(\tau) - \delta(\tau))d\tau$.

averaged ones. By evaluating the time averaging (on a dither period) of both the input and output signals of the step nonlinearity during different dynamic operating conditions, Fig. 13 is obtained. The computed averaged nonlinearities reproduce their analytical prediction obtained through (12). Indeed it is also possible to show that the averaged system approximates quite well the behavior of the dithered system, although the condition (ii) of Proposition 3.1 is violated. This is not true in general, as it was shown in Proposition 6.2 and as it will be confirmed by the next experiment.

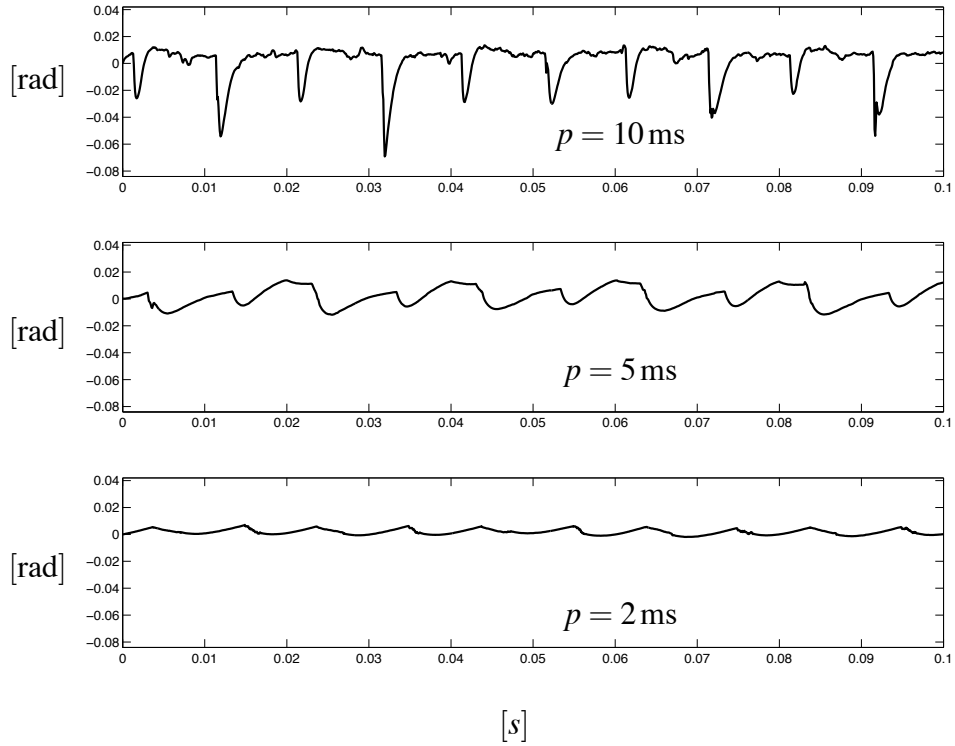

Fig. 14. Measured angular position x_1 for sawtooth dither of three frequencies.

7.2 H-bridge drive

Consider the DC motor control system described in Section 2.2. The DC motor has the following parameters: $R_a = 2.510\,\Omega$, $L_a = 0.530\,\mathrm{mH}$, $k_t = k_e = 5.700\,\mathrm{mV}/(\mathrm{rad}\cdot \mathrm{s}^{-1})$, $\beta = 0.411\,\mathrm{mN}\cdot\mathrm{cm}/(\mathrm{rad}\cdot\mathrm{s}^{-1})$, $J = 31.400\,\mathrm{g}\cdot\mathrm{cm}^2$, $k_{\mathrm{pot}} = 3/(2\pi)\mathrm{V/rad}$, $v = 4.500\,\mathrm{V}$. Two dither shapes are considered: a sawtooth signal and a trapezoidal signal. The dither amplitude is in all cases equal to $M_\delta = 70\mathrm{mV}$. It can be shown (e.g., using the Popov criterion) that the averaged systems corresponding to the sawtooth and trapezoidal dither cases are both asymptotically stable. For sawtooth dither, the approximation error between the dithered system and the averaged system tends to zero as the dither frequency goes to infinity, in accordance with Proposition 3.1. Hence, since the averaged system is asymptotically stable, the system output goes to zero as we increase the dither frequency. For trapezoidal dither, the assumptions of Proposition 3.1 are not fulfilled, since trapezoidal dither has a discontinuous amplitude distribution function.

The following DC motor experiments support these theoretical conclusions. The system is stabilized with sawtooth dither, but not with trapezoidal dither. Experiments were carried out using sawtooth dither of frequencies 100, 200, and 500 Hz. Fig. 14 reports the angular position of the motor shaft under steady-state conditions and Fig. 15 a phase-space diagram. Note that by increasing the dither frequency the

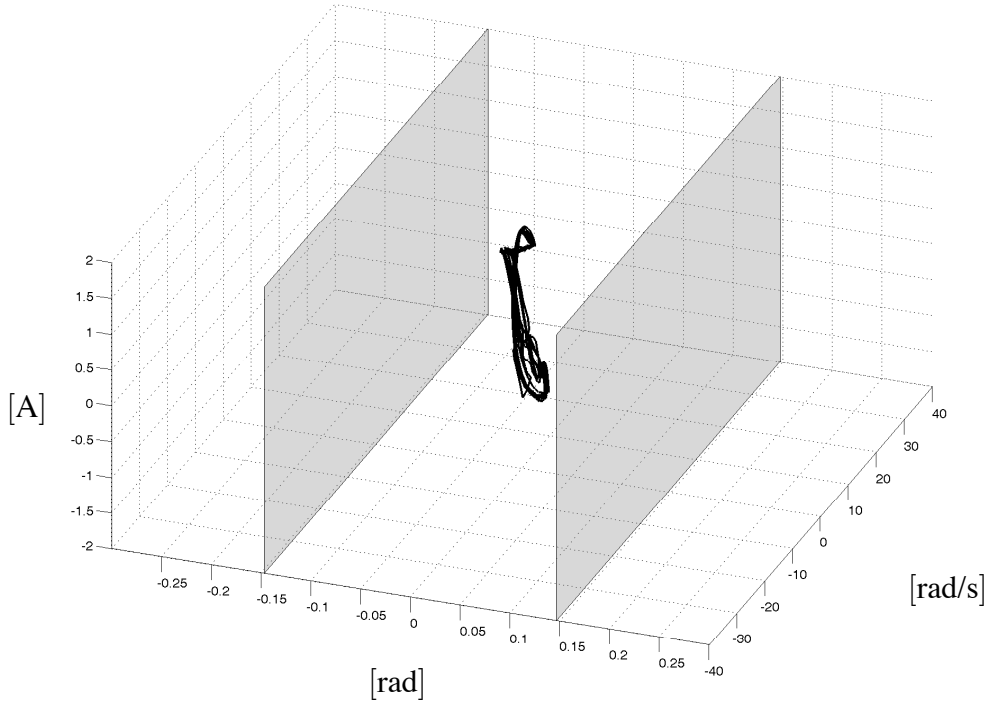

Fig. 15. Phase-space with sawtooth dither with $p = 5$ ms: the armature current, the measured angular position and the angular speed. Note that the angular position has a small ripple as illustrated in Fig. 14. The two planes reported in the figure represent the boundaries corresponding to the minimum and maximum values of the dither.

behavior of the dithered system converges to the behavior of the (stable) averaged system (i.e., the system output goes to zero). Table 2 reports the ratios between consecutive averages of the peak-to-peak values of the output signal, thus indicating the convergence rate. The averaging effect of the dither works properly in this case. Figs. 16–17 show experiments with trapezoidal dither. In this case, the system output shows a slow oscillation with a substantial amplitude for all three dither frequencies. The frequency of the oscillation is low compared to the dither frequency, and it seems to be relatively independent of the dither frequency. In particular, note that by increasing the dither frequency, the system output does not converge to zero, as was the case with sawtooth dither. Instead going from 200 Hz to 500 Hz, the amplitude of the oscillation is even increasing, see Table 2.

To investigate the high frequency limiting case, a square wave dither of 1 MHz has been applied. Fig. 18 shows the result. Although the trajectory does not intersect the planes in this case, the dither still does not stabilize the system about the origin.

The oscillations that appear in Figs. 16–18 are not predicted by the averaged dynamics. The oscillations in the experiments also appear in simulations of the corresponding dithered system and it is an example of the discrepancy that may appear

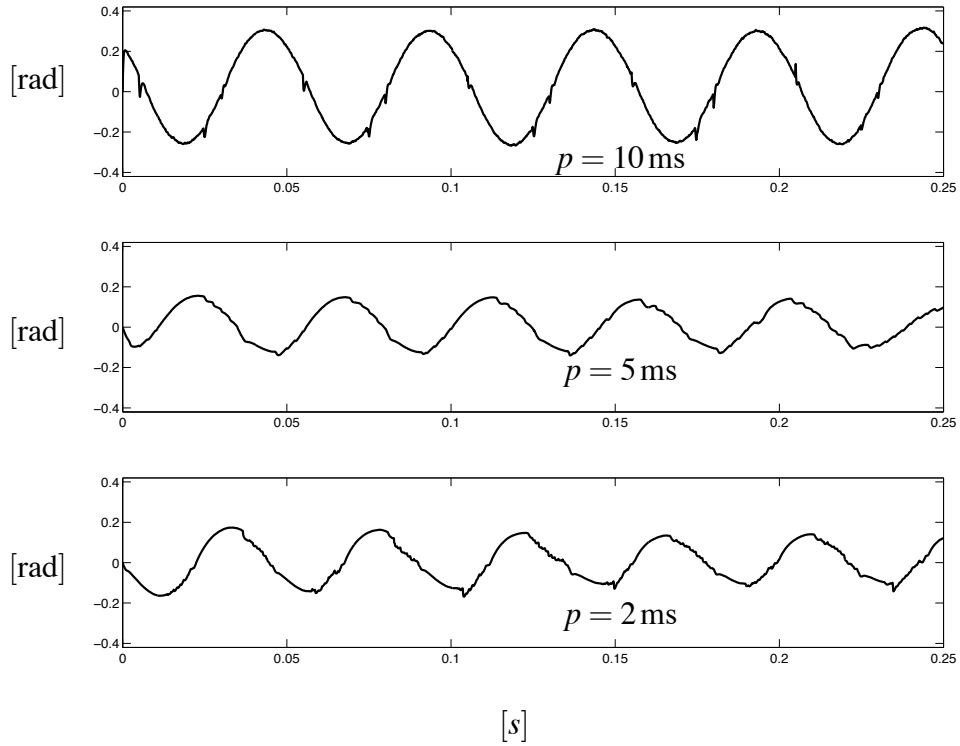

Fig. 16. Measured angular position for trapezoidal dither of three frequencies. Note the different scale compared to Fig. 14.

between the solutions of the dithered and averaged systems when the conditions of the averaging theorem are not satisfied.

8 Conclusions

In this paper it has been shown that an important class of power electronics systems can be re-casted in the framework of dithered nonsmooth systems. By exploiting recent theory for hybrid systems with external excitation, it has been analyzed how

	Sawtooth dither		Trapezoidal dither	
f	peak-to-peak	ratio	peak-to-peak	ratio
100 Hz	0.0850 rad	3.32	0.582 rad	1.97
200 Hz	0.0256 rad	2.84	0.295 rad	0.86
500 Hz	0.0090 rad	-	0.343 rad	-

Table 2
Experimental results of the angular position for the H-bridge drive with different dither signals.

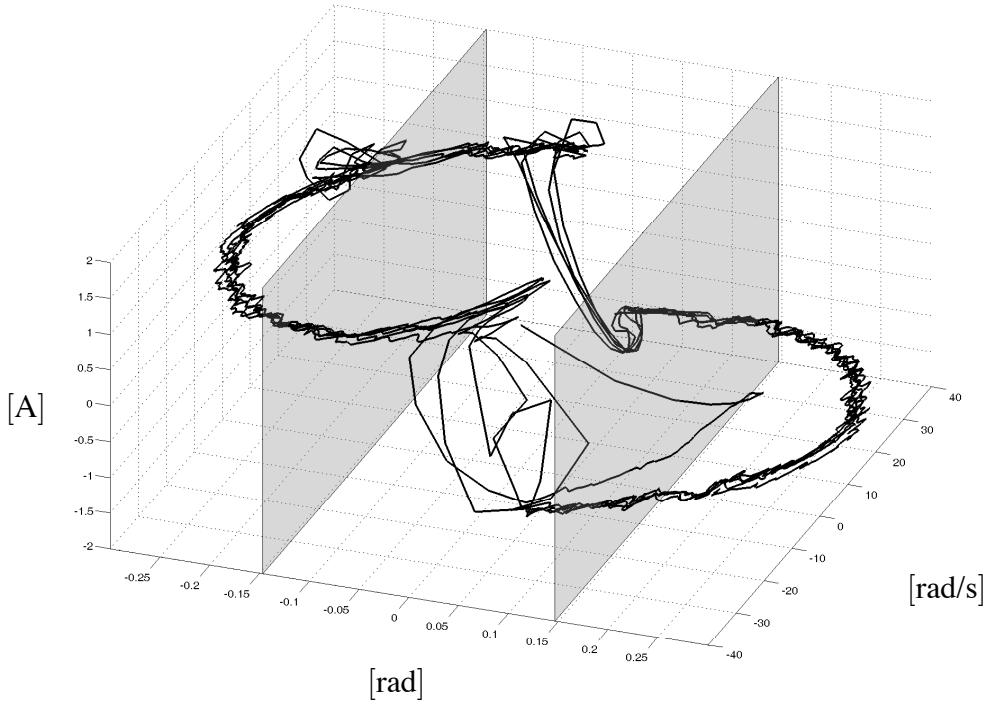

Fig. 17. Phase-space with trapezoidal dither with $p = 10\,\text{ms}$.

the shape of the external signal affects the averaging result and thereby the behavior of the power converters. Simulations and experiments supported the theoretical results and showed the importance of understanding the limitations of averaging theory in practice.

The results presented in this paper propose several interesting research problems for future investigations. An important problem is on developing principles for dither design. The paper shows that certain classes of dither signals are more suitable than others. A next step would be to optimize the choice of signal within such a class. For practical problems, such as the design of power converters, implementation aspects should be taken into account in this procedure, since certain modulation signals might be easier to generate or are more desirable for other reasons. Further analysis of some of the dynamical properties illustrated in the simulations and experiments of the paper is needed. For instance, the peculiar oscillations that appear in the experiments of the H-bridge drive with trapezoidal dither require further investigations.

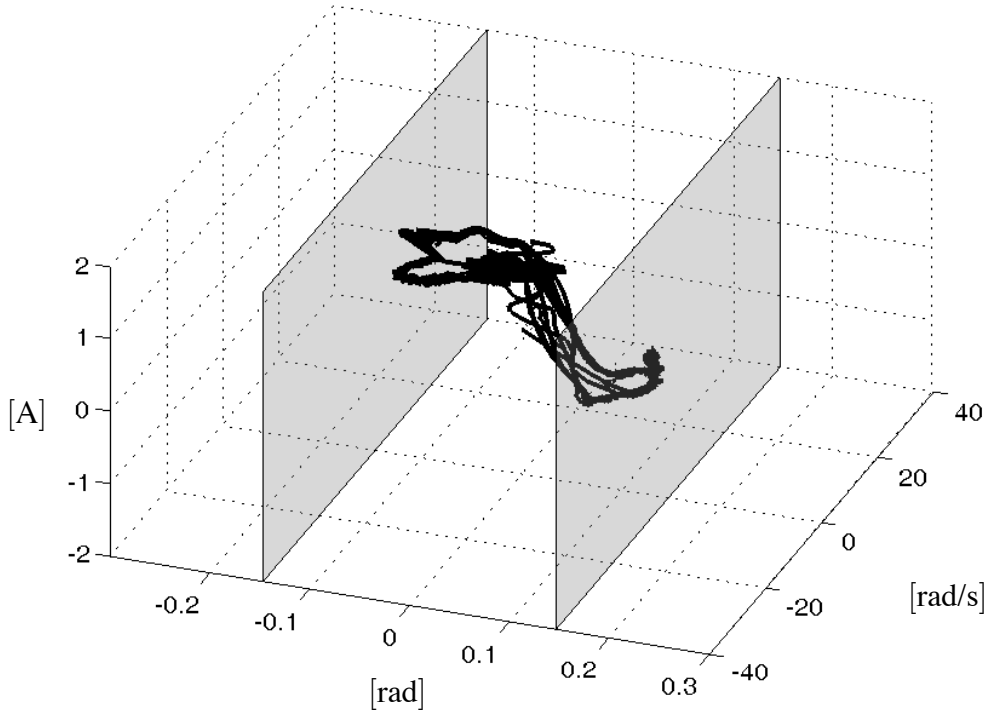

Fig. 18. Phase-space with square wave dither with $p = 1\,\mu$s.

9 Acknowledgements

Authors would like to acknowledge Roberto Frasca, Luca Piedimonte and Vittorio Sandoli for their help in the experiments.

References

Banerjee, S. and Verghese, G. C., Eds. (2001). *Nonlinear Phenomena in Power Electronics: Bifurcations, Chaos, Control, and Applications*. Wiley-IEEE Press. New York.

Escobar, G., A.J. van der Schaft and R. Ortega (1999). A hamiltonian viewpoint in the modelling of switching power converters. *Automatica* **35**(3), 445–452.

Gelig, A. Kh. and A. Churilov (1998). *Stability and Oscillations of Nonlinear Pulse Modulated Systems*. Birkhäuser. Berlin.

Guéguen, H. and J. Zaytoon (2004). On the formal verification of hybrid systems. *Control Engineering Practice* **12**(10), 1253–1267.

Iannelli, L., K. H. Johansson, U. Jönsson and F. Vasca (2003). Dither for smoothing relay feedback systems: an averaging approach. *IEEE Trans. on Circuits and Systems, Part I* **50**(8), 1025–1035.

Iannelli, L., K. H. Johansson, U. Jönsson and F. Vasca (2004). On the averaging of a class of hybrid systems. In: *Proc. of IEEE Conference on Decision and Control*. Vol. 2. Bahamas. pp. 1400–1405.

Iannelli, L., K. H. Johansson, U. Jönsson and F. Vasca (2006). Averaging of nonsmooth systems using dither. *Automatica* **42**(4), 669–676.

Jönsson, U. and A. Megretski (2000). The Zames Falb IQC for systems with integrators. *IEEE Trans. on Automatic Control* **45**(3), 560–565.

Kassakian, J. G., M. F. Schlecht and G. C. Vergese (2001). *Principles of Power Electronics*. Prentice-Hall. Reading, MA.

Lehman, B. and R. Bass (1996). Extensions of averaging theory for power electronics systems. *IEEE Trans. on Power Electronics* **11**(4), 542–553.

Liberzon, D. (2003). *Switching in Systems and Control*. Birkhäuser. Boston, USA.

Lygeros, J., K. H. Johansson, S. N. Simić, J. Zhang and S. Sastry (2003). Dynamical properties of hybrid automata. *IEEE Trans. on Automatic Control* **48**(1), 2–17.

Megretski, A. and A. Rantzer (1997). System analysis via integral quadratic constraints. *IEEE Trans. on Automatic Control* **42**(6), 819–830.

Mohan, N., T. M. Undeland and W. P. Robbins (1995). *Power electronics: converters, applications, and design*. John Wiley and Sons, Inc.. New York.

Moreau, L. and D. Aeyels (2000). Practical stability and stabilization. *IEEE Trans. on Automatic Control* **45**(8), 1554–1558.

Ortega, R., A. Loria, P. J. Nicklasson and H. Sira-Ramirez (1988). *Passivity-Based Control of Euler-Lagrange Systems: Mechanical, Electrical and Electromechanical applicatio ns*. Springer.

Teel, A., L. Moreau and D. Nesic (2004). Input-to-state set stability of pulse width modulated systems with disturbances. *Systems and Control Letters* **51**(1), 23–32.

Zames, G. and N. A. Shneydor (1976). Dither in non-linear systems. *IEEE Trans. on Automatic Control* **21**(5), 660–667.

Zames, G. and N. A. Shneydor (1977). Structural stabilization and quenching by dither in non-linear systems. *IEEE Trans. on Automatic Control* **22**(3), 352–361.

Zames, G. and P. L. Falb (1968). Stability conditions for systems with monotone and slope-restricted nonlinearities. *SIAM Journal of Control* **6**(1), 89–108.

Appendix: Proofs

Proof of Proposition 4.1

To prove the result iteratively consider time intervals of length $T = -\alpha_0{}^{-1}\ln(\alpha_1/\beta_0)$ where $0 < \alpha_1 < 1$. Let $\varepsilon_0 = \gamma p_0$, where $\gamma = \gamma(\mathcal{K}, T)$. Then Proposition 3.1 implies

$$|x(t) - w(t)| \leq \varepsilon_0$$

on $t \in [0, T]$. By considering a sequence of functions $\tilde{w}_k$, $k = 1, 2, \ldots$, each defined on an interval $[kT, (k+1)T]$ and satisfying (11) with $\tilde{w}_k(kT) = x(kT)$, then it follows that

$$|\tilde{w}_k(t) - w^0| \leq \beta_0 e^{-\alpha_0(t-kT)}|x(kT) - w^0|, \quad \forall t \geq kT,$$

and, by applying Proposition 3.1 again,

$$|x(t) - w^0| = |x(t) - \tilde{w}_k(t) + \tilde{w}_k(t) - w^0| \leq \beta_0 e^{-\alpha_0(t-kT)}|x(kT) - w^0| + \varepsilon_0 \quad (21)$$

on $t \in [kT, (k+1)T]$. By evaluating (21) in $t = (k+1)T$,

$$\left|x((k+1)T) - w^0\right| \leq \alpha_1 |x(kT) - w^0| + \varepsilon_0. \quad (22)$$

Hence

$$\left|x(kT) - w^0\right| \leq \alpha_1^k \left|x_0 - w^0\right| + \varepsilon_0 \frac{1 - \alpha_1^k}{1 - \alpha_1}. \quad (23)$$

Then (21) becomes

$$\begin{aligned} |x(t) - w^0| &\leq \beta_0 e^{-\alpha_0(t-kT)} \left(e^{-\alpha kT} |x_0 - w^0| + \frac{\varepsilon_0}{1 - \alpha_1} \right) + \varepsilon_0 \\ &\leq \beta_0 e^{-\alpha t} \left|x_0 - w^0\right| + \beta_0 \frac{\varepsilon_0}{1 - \alpha_1} + \varepsilon_0, \end{aligned} \quad (24)$$

for $t \in [kT, (k+1)T]$, where $\alpha = -T^{-1}\ln\alpha_1$, which implies $\alpha < \alpha_0$. The result follows since (24) is valid for any k and

$$\beta_0 \frac{\varepsilon_0}{1 - \alpha_1} + \varepsilon_0 = \gamma p_0 \frac{\beta_0 + 1 - \alpha_1}{1 - \alpha_1} = \varepsilon.$$

Proof of Proposition 4.2

Condition (i) and (iii) implies by the Kalman-Yakubovich-Popov Lemma that there exists $P = P^T > 0$ such that

$$\begin{bmatrix} A^T P + PA + 2\alpha P + 2\alpha\lambda k c^T c & Pb - (c(I - \lambda A))^T \\ b^T P - c(I - \lambda A) & -\frac{2}{k} - 2\lambda cb \end{bmatrix} \leq 0 \tag{25}$$

Let $z = w - w^0$, $y = -c(w - w^0)$, $\phi(y) = N(r - cw^0 + y) - N(r - cw^0)$. Then the error dynamics satisfies

$$\dot{z} = Az + b\phi(y), \qquad y = -cz$$

and by (ii) the following sector condition holds $(y - \frac{1}{k}\phi(y))\phi(y) \geq 0$. Let $V_0(z) = z^T Pz$ and

$$V(z) = V_0(z) + \lambda \int_0^y \phi(\sigma) d\sigma$$

It follows from (14) that the nonlinearity is monotonically nondecreasing (because F_δ is monotonically nondecreasing), which in turn implies that the integral always is positive. This implies that this Lyapunov candidate is bounded by

$$\lambda_{\min}(P)|z|^2 \leq V(z) \leq \left(\lambda_{\max}(P) + \frac{\lambda k}{2}|c|^2\right)|z|^2 \tag{26}$$

Finally, from (25) and the sector condition on ϕ it can be derived the following bound on the derivative

$$\dot{V}(z) \leq -2\alpha V(z) \tag{27}$$

It follows from (26) and (27) that $|z(t)| \leq \beta e^{-\alpha t}|z(0)|$, where

$$\beta = \sqrt{(\lambda_{\max}(P) + \lambda k|c|^2/2)/\lambda_{\min}(P)}.$$

This completes the proof.